SOI: 1.1/TAS DOI: 10.15863/TAS
International Scientific Journal
Theoretical & Applied Science

p-ISSN: 2308-4944 (print) **e-ISSN:** 2409-0085 (online)

Year: 2025 **Issue:** 02 **Volume:** 142

Published: 26.02.2025 http://T-Science.org

Issue Article

S. M. Zainab
Al-Muthanna University
College of Science, Physics Department
Zainab.lahmod@mu.edu.iq

A. A. Alaakol
Al-Muthanna University
College of Science, Physics Department
ashwaq.alaakol@gmail.com

ELECTROMAGNETIC STRUCTURE OF $N_\rho = 10$ BOSONS IN THE FRAME WORK OF IBM-2

Abstract: *This study used the IBM-2 variant of the approximation of interacting bosons to examine the level structure of $^{100}_{40}Zr$ and $^{76}_{36}Kr$. The energy levels of the two nuclei were computed, resulting in the formulation of a decay plan. The matrix elements provide the origin of the electromagnetic characteristics. This study examines the mixing ratios of transitions connecting the gamma, beta, and ground state bands. The transition ratios have been assessed. The anticipated theoretical calculations were juxtaposed with the experimental results shown in the corresponding figures and tables. The experimental data aligns with the expected outcomes.*

Key words: *Interacting boson approximation, Isotopes even – even ($^{100}_{40}Zr$, $^{76}_{36}Kr$), qaudrupole moments, mixing ratios, energy levels, $N_\rho = 10$ bosons, Electromagnetic transitions probabilities, Electric monopole transitions.*

Language: *English*

Citation: Zainab, S.M., & Alaakol, A.A. (2025). Electromagnetic Structure of $N_\rho = 10$ Bosons in the frame work of IBM-2 . *ISJ Theoretical & Applied Science, 02 (142),* 91-97.

Soi: https://s-o-i.org/1.1/TAS-02-142-16 ***Doi***: crossref https://dx.doi.org/10.15863/TAS.2025.02.142.16

Scopus ASCC: *3100.*

Introduction

The transitional nuclear regions, including the nuclei, consistently provide a challenge to both experimental and theoretical nuclear physicists. This is attributable to the asymmetry feature present in the decay schemes of the majority of nuclei in this area [1,2]. The Interacting Boson Model is expected to provide an appropriate characterisation of the nuclear structure of nuclei in this domain [3,4]. This study begins with the selection of nuclei that exhibit a certain relationship, such as an equivalent boson number beyond the closed shell at N=Z=28 or 50. Both selected isotopes possess a total of 10 bosons external to the closed shell. The isotopic series seen in fig-1, to which these two nuclei are associated, has been the subject of several theoretical investigations using various models[5,6,7,8] . These two nuclei possess a characteristic of being in proximity to the ground state, exhibiting the third excited state, and decaying via two types of transitions as seen in fig-2. The Zr isotope A=100 is significant as it represents the transition from the subshell closure at N=58 to the filling of the $h_{11/2}$ subshell and exhibits substantial deformation [9]. The objectives of the current study are enumerated as follows:

1. To do systematic calculations for nuclei inside this area
2. Select the optimal parameters to ensure that the computed values closely align with the experimental data and extrapolate IBM-1 calculations to IBM-2.
3. To delineate the principal electromagnetic characteristics of these isotopes.

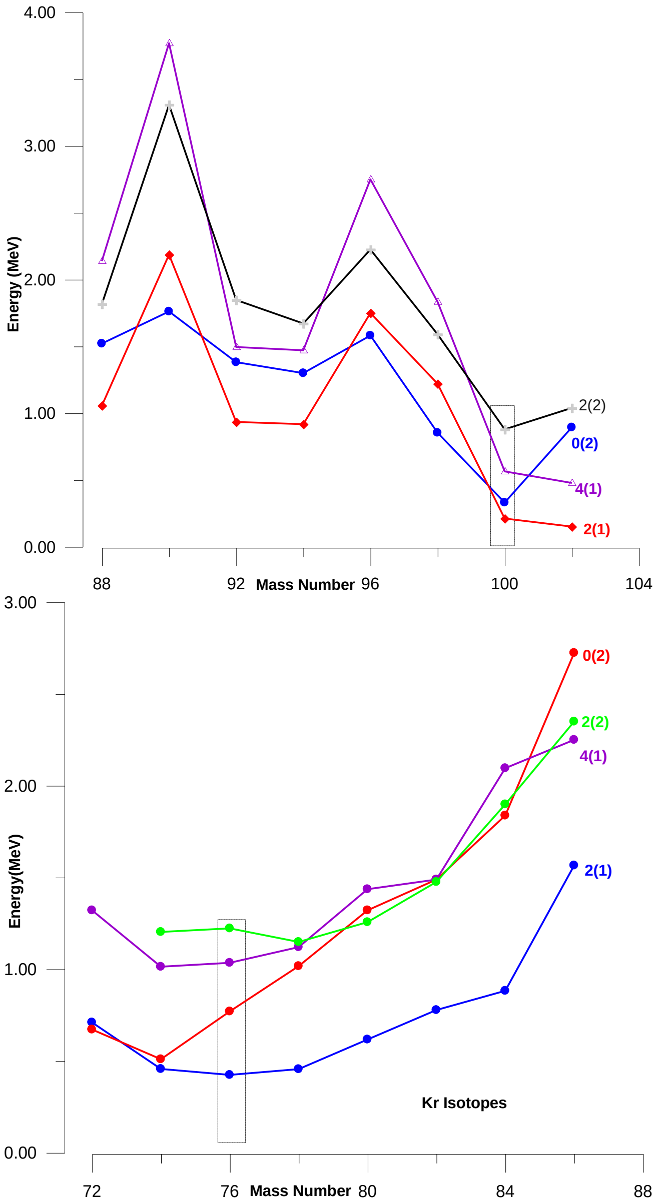

Fig 1: Systematics of experimental energy levels of Zr and Kr isotopes [9], delineating the region of research with dotted lines in both panels.

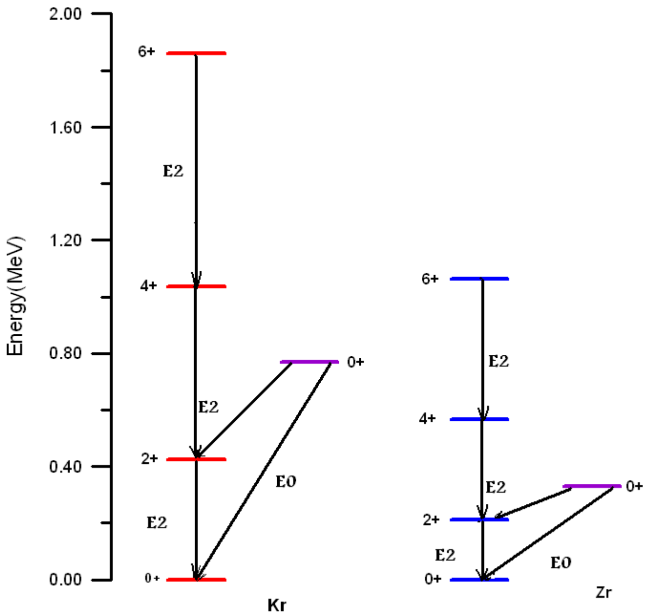

Fig 2: The experimental decay of 0+ states in the two nuclei [9].

1. The model

In the IBM-2 Hamiltonian, the S and D pairs of valence nucleons possess angular momentum J=0 and J=2, respectively. These pairings intuitively correspond to the s and d bosons, respectively. The fundamental components of the IBM-2 are proton bosons and neutrons. The Hamiltonian expressed as

$H = \varepsilon_d(\hat{n}_{d\nu} + \hat{n}_{d\pi}) + k(\hat{Q}_\nu.\hat{Q}_\pi) + V_{\nu\nu} + V_{\pi\pi} + M_{\nu\pi}$ (1)

in which the dot represented the scalar product. The first component (ε_d)stands for the energies of the single bosons of neutrons and protons, indicates the difference in energy between the *s* and *d* bosons, and is the quantity of d-bosons, where d-bosons correspond to bosons of proton or neutron, respectively [10,11]. The quadrupole-quadrupole interaction between neutron and proton bosons, with a strength of, is the second component that indicates the primary portion of the boson-boson interaction. The operator with four quadrants is

$Q_\rho = [d_\rho^+ s_\rho + s_\rho^+ \tilde{d}_\rho]^2 + \chi_\rho [d_\rho^+ \tilde{d}_\rho]^2 \quad \rho = \nu \; or \; \pi$ (2)

Where χ_ρ is an experimentally established parameter that defines the quadrupole operator's structure. Eq (2) uses the symbol "angular momentum coupling" in the square bracket. In order to enhance the fit to experimental energy spectra, it is sometimes necessary to incorporate the variables $V_{\nu\nu}$ and $V_{\pi\pi}$ in eq (1), which represent the interaction of like-bosons [12]. They take the form

$V_\rho = \frac{1}{2}\sum_{L=0,2,4} C_L^\rho \left([d_\rho^+ d_\rho^+]^L . [\tilde{d}_\rho \tilde{d}_\rho]^L\right)$ (3)

To simplify, one may reduce the number of free parameters C_L^ρ by imposing the condition

$C_L^\pi = C_L^\nu = C_L$.

The Majorana term, $M_{\nu\pi}$, including three factors ζ_1, ζ_2, and ζ_3, may be expressed as

$M_{\nu\pi} = \frac{1}{2}\zeta_2([s_\nu^+ d_\pi^+ - d_\nu^+ s_\pi]^2.[s_\nu \tilde{d}_\pi - \tilde{d}_\nu s_\pi]^2 -) - \sum_{k=1,3}\zeta_k([d_\nu^+ d_\pi^+]^k.[\tilde{d}_\nu \tilde{d}_\pi]^k)$ (4)

The B(E2) values were computed with the operator

$T^{(E2)} = \alpha_{2\rho}(d^+ \times s + s^+ \times d^\sim)_\rho^2 + \beta_{2\rho}(d^+ \times d^\sim)_\rho^1$ (5)

It may be expressed in shorthand as a quadruple electric operator as follows:

$T^{(E2)} = e_\pi Q_\pi + e_\nu Q_V$ (6)

In this context, $Q_{\pi,\nu}$ is identical to that in eq (2), whereas e_π and e_ν represent boson effective charges that are contingent upon the boson number N_ρ, and they may assume any value to align with the experimental outcomes [13]. The transition operator for the magnetic dipole $M1$ may be expressed as follows:

$T^{(M1)} = \sqrt{\frac{3}{4\pi}}(g_\pi L_\pi^{(1)} + g_\nu L_\nu^{(1)})$ (7)

Where g_π, g_ν are the gyromagnetic coefficients of the proton and neutron respectively in μ_n units and $L_\rho^{(1)} = \sqrt{10}[d^+ \times d^\sim]^{(1)}$[14]. Thus, the $T^{(M1)}$ operator can be written as follows:

$T^{(M1)} = \sqrt{\frac{3}{4\pi}}\left[\frac{1}{2}(g_\pi + g_\nu)(L_\pi^{(1)} + L_\nu^{(1)}) + \frac{1}{2}(g_\pi - g_\nu)(L_\pi^{(1)} - L_\nu^{(1)})\right]$ (8)

The first term of the aforementioned equation is diagonal; hence, the equation may be reformulated in terms of boson operators as follows:

$$T^{(M1)} = 0.77[(d^+ \times d^\sim)^1_\pi - (d^+ \times d^\sim)^1_\nu](g_\pi - g_\nu) \quad (9)$$

The electromagnetic transitions of the nucleus are often impure; for instance, a level may be broadened by an electromagnetic transition, an electric quadrupole, or a magnetic dipole. This phenomenon arises from mixed symmetry (MSSs)[15]. To determine which of the two transitions is predominant, it is essential to understand the concept of the mixing ratio, represented by the following formula:

$$\delta\left({}^{E2}/_{M1}\right) = 0.85E_\gamma.\Delta \quad (10)$$

E_γ is the gamma energy of the transition measured in MeV, and Δ is determined by the relation

$$\Delta = \frac{\langle J_f | T^{(E2)} | J_i \rangle}{\langle J_f | T^{(M1)} | J_i \rangle} \quad (11)$$

2. Results and discussion

2.1 Parameters

To identify the Zr and Kr on the IBM-2 parameters map, it is necessary to analyse certain specific aspects of these nuclei. The number of nucleons outside the magic closed shell at 50 consists of 10 proton holes for zirconium (Zr) and 8 for krypton (Kr), whereas the neutron particles are 10 for Zr and 12 for Kr, respectively. The total boson number in each isotope is N=10. We possess two nuclei characterised by distinct quantities of valence neutrons and protons, with the experimental ratios $R_1 = E_{41}/E_{21}$ for Kr being 2.44 and for Zr 2.66, $R_2 = E_{61}/E_{21}$ for Kr 4.38 and for Zr 4.98, and $R_3 = E_{02}/E_{21}$ for Kr 1.82 and for Zr 1.56. All these qualities indicate that these nuclei possess identical characteristics. Table-1 is a compilation of the IBM-2 parameters.

Table-1. The IBM-2 Parameters

Nucleus	N_π	N_ν	N	ε	κ	χ_π	χ_ν	$C_{0,2,4}$	$\xi_1 = \xi_3, \xi_2$
${}^{76}_{36}Kr$	4	6	10	0.94	-0.08	-0.8	-1.2	-1.0, 0.2, 0.05	0.27,0.055
${}^{100}_{40}Zr$	5	5	10	0.81	-0.21	-0.9	-0.92	0.75,0.05,0.05	-0.225, -0.02

The factors $C_{0,2,4}$ significantly affect the energy of 0_2, which is about 2_1 in both nuclei. The parameters of Dejakhsh et al. [16] were used for the nucleus ${}^{76}_{36}Kr$, with minor adjustments made to enhance concordance. In the instance of ${}^{100}_{40}Zr$, the parameters varied in accordance with the energy of the 2_1, making it challenging to get optimal outcomes. However, it is seen that the little variation in energy values has a negligible impact on the transition matrix components of high-energy states.

2.2 Excitation Energies

The results of the energy level calculations are shown in Table-2. The chart clearly indicates that the fit for Kr is much superior than that for ${}^{100}_{40}Zr$. Nonetheless, the model is proficient in accurately calculating the energy level 0_2. The largest variance from experimental data is 0.345 MeV for the 8^+ state of ${}^{76}_{36}Kr$, which is generally acceptable for high-energy states. However, the overall results are rather satisfactory.

Table-2. Experimental and theoretical values of energy levels for ${}^{76}_{36}Kr$ and ${}^{100}_{40}Zr$

Nucleus	Values	2_1	4_1	6_1	8_1	0_2	2_2	4_2
^{76}Kr	Exp.	0.424	1.035	1.859	2.878	0.770	1.222	1.957
	IBM-2	0.433	1.022	1.761	2.637	0.774	1.242	1.944
^{100}Zr	Exp.	0.213	0.566	1.069	1.689	0.331	0.879	1.414
	IBM-2	0.212	0.667	1.291	2.035	0.381	0.552	0.923

To assess the extent of collectivity in the level schemes of both nuclei, one must compute the ratios that include the band head of the β_1 and γ_1 isotopes [17,18].

$$R_{2,0,\beta,g} = \frac{E(2^+_\beta) - E(0^+_\beta)}{E(2^+_1)}, \quad R_{4,2,\beta,g} = \frac{E(4^+_\beta) - E(2^+_\beta)}{E(4^+_1) - E(2^+_1)},$$

$$R_{4,2,\gamma,g} = \frac{E(2^+_\beta) - E(0^+_\beta)}{E(4^+_1) - E(2^+_1)}$$

the results are listed in Table- 3.

Table-3. Comparison between the ratios R_1 , R_2 and R_3

Nucleus	Values	R_1	R_2	R_3
^{76}Kr	**Experimental**	1.066	1.203	0.728
	Theoretical	1.080	1.192	0.794
^{100}Zr	**Experimental**	2.573	1.515	1.552
	Theoretical	0.806	0.815	0.378

2.3 electromagnetic transitions probabilities and moments

The matrix element of the E2 operator from Eq. (6) has been computed using the effective charges for both nuclei$e_\pi = 0.075eb$ and$e_\nu = 0.090eb$ .Table(3) presents some significant lowered E2 transition probabilities. The effective charges were selected to ensure a strong correlation with the transition from the initial excited state over the examined area. The general concordance with existing experimental data is excellent.

Table-4. Experimental and theoretical values of electric quadrupole reduced transition probability of ^{76}Kr and ^{100}Zr nuclei.

Transition	^{76}Kr		^{100}Zr	
	exp.	th.	exp.	th
$B(E2;2_1-0_1)$	0.164(6)	0.163	0.21(2)	0.224
$B(E2;4_1-2_1)$	0.198(20)	0.276	0.28(3)	0.294
$B(E2;6_1-4_1)$	0.177(15)	0.316	0.38(6)	0.240
$B(E2;2_2-0_1)$	0.009	0.002	-	0.004
$B(E2;2_2-2_1)$	0.004	0.059	-	0.005
$B(E2;0_2-2_1)$	-	0.175	0.184	0.004
$B(E2;2_3-0_1)$	-	0.002	-	0.012
$B(E2;2_3-2_1)$	-	0.030	-	0.000
$B(E2;3_1-2_1)$	-	0.000	-	0.004
$B(E2;1_1-0_1)$	-	0.000	-	0.000
$B(E2;3_1-1_1)$	-	0.000	-	0.142
$B(E2;4_2-4_1)$	0.001	0.029	-	0.003
$B(E2;4_2-2_2)$	0.086(30)	0.181		0.013

2.4 Electric quadrupole moment

The 2_1^+ electric quadrupole moments were anticipated. Due to its unavailability, it may be computed utilising the relationship pertaining to the distorted nuclei as outlined in reference [19].

$$B(E2;0--2) = \frac{5}{16\pi}Q_0^2 Q(2_1^+) = -\frac{2}{7}Q_o \qquad (12)$$

Where Q_0 represents the static quadrupole moment. The findings are shown in Table 5. The predicted values consistently exceeded one and had the same negative sign as the experimental values.

Table-5. The values of electric qaudrupole moments of the isotones N=88

Nucleus	$[Qefm^2]_{exp.}$	$[Qefm^2]_{theor.}$
$^{76}Kr_{36}$	0.82(3)	-0.99
$^{100}Zr_{40}$	0.93(9)	-1.26

2.5 The M1 transition and mixing ratio $\delta(E2/M1)$

To anticipate the diminished M1 matrix components using eq (7), one must evaluate the values of g_π and g_ν. Sambataro and Dieperink shown that the overall experimental g factor of the 2_1level exhibits a straightforward linear correlation with g_π and g_ν, expressed as follows [20];

$$g = g_\pi \frac{N_\pi}{N_\pi+N_\nu} + g_\nu \frac{N_\nu}{N_\pi+N_\nu} \qquad (13)$$

The magnetic moment of the Zr nucleus is $\mu = 0.56(7)nm$, and from $\mu = 2g$, the relation $g_\pi + g_\nu = 0.56$is derived [21]. The estimated values of $g_\pi = 0.19 and g_\nu = 0.37$are used to compute the M1 matrix elements using eq (10). The M1 matrix and E2 matrix components were amalgamated in the computation of the mixing ratio $\delta(E2/M1)$ via the relation;

$$\delta(E2/M1) = 0.835E_\gamma(MeV) \times \frac{T(E2)}{T(M1)} \qquad (14)$$

Table-6. A comparison between available experimental of $\delta(E2/M1)$ and IBM-2 prediction

Nucleus	Values	$\delta(E2/M1;2_2-2_1)$	$\delta(E2/M1;2_3-2_1)$	$\delta(E2/M1;4_2-4_1)$
Kr	**Experimental**	+0.2(1)	-	-0.84(5)
	Theoretical	-4.033	+37.52	-2.96

Zr	**Experimental**	+1.0(3)	-	-
	Theoretical	+0.17	-3.44	-34.56

Table 6 illustrates the discrepancy between the experimental data and the computed values, particularly in the case of $\delta(E2/M1; 2_2 - 2_1)$. Nonetheless, the minor experimental value, 0.2(1), suggests a diminutive magnitude of E2 matrix elements, while the literature [13] reports the E2 decreased transition probability as 2.0 w.u and M1 as 0.024 w.u, resulting in a mixing ratio much beyond 1, consistent with model predictions.The same rationale applies to the transition $4_2 \to 4_1$, which exhibits B(E2)=11(4) w.u. and B(M1)=0.009(35) w.u., whereas the experimental mixing ratio is -0.84(5), as shown in the table.

2.6 The X (E0/E2) Ratio

The E0 transition transpires between two states of identical spin and parity, facilitating the passage of energy without any angular momentum and without competing gamma radiation. When a surface alteration occurs in the nucleus, the E0 transition is present. In nuclear models that assume a fixed surface, E0 transitions are strongly prohibited, as shown in the shell and IBM-1 models. Electric monopole transitions may occur in $0^+ \to 0^+$ transitions, as well as in competition with gamma multipole transitions. Depending on the selection criteria for transitions, they may also compete in any $\Delta I = 0$ decay, such as $2^+ \to 2^+$ or any $I_i = I_f$ states within the framework. Monopole pair generation is feasible with transition energy above $2m_o c^2$. The E0 reduced transition probability is denoted as [22,23].

$$B(E0; I_i - I_f) = e^2 R^4 \rho^2(E0) I_i = I_f \qquad (15)$$

where e denotes the electronic effective charge, R represents the nuclear radius, and $\rho(E0)$ signifies the transition matrix element. Nonetheless, there are only a few instances when $\rho(E0)$ may be directly measured. In most instances, we must ascertain the intensity ratio of E0 to the competing E2 transition, referred to as the $X(\frac{E0}{E2})$ value [24]. It may be expressed as

$$X(E0/_{E2}) = \frac{B(E0; I_i - I_f)}{B(E2; I_i - I_{f'})} \qquad (16)$$

Where $I_f = I_{f'}$ for $I_i \neq 0, and I_f = 0, I_{f'} = 2 for I_i = 0$. The $T^{(E0)}$ operator my be found by setting $l = 0$on the IBM-2 operator [25,26].

$$\rho_{if}(E0) = \frac{Z}{{R_0}^2} \sum \tilde{\beta}_{0\rho} \langle f | d^+{}_\rho x d_\rho | i \rangle \qquad (17)$$

where $R_0=1.2A^{1/3}$ fm and $\rho(E0)$ is a dimensionless quantity. The two parameters $\tilde{\beta}_{0\pi}, \tilde{\beta}_{0\nu}$ in equation (12) may be estimated by fitting in isotope shift, which is the difference in the square radius $\delta\langle r^2 \rangle$ between neighboring isotopes in their ground state [27,28]. i.e.

$$\delta\langle r^2 \rangle = \langle 2_1{}^+ | T_0 | 2_1{}^+ \rangle - \langle 0_1{}^+ | T_0 | 0_1{}^+ \rangle. \qquad (18)$$

The results of calculation are presented in Table-7.

Table-7. A comparison between available experimental data and model prediction of $X(E0/E2)$ ratio.

Nucleus	Values	$X(E0/E2; 2_2 - 2_1)$	$X(E0/E2; 0_2 - 0_1)$	$X(E0/E2; 0_3 - 0_1)$
Kr	**Experimental**	-	-	-
	Theoretical	0.035	0.211	3.56
Zr	**Experimental**	-	0.060(11)	-
	Theoretical	0.044	0.113	5.68

Conclusion

The nuclear structure of two nuclei has been studied. Each of these nuclei contains the same number of bosons, which come from different closed shells. This research improves the theoretical knowledge of both isotopes in terms of energy levels, reduced transition probabilities, and their mixing. The results of IBM-2 show a strong connection with the experimental data that is currently available. It has been decided that further experimental data are required in order to conduct a comprehensive investigation of the level structure of these nuclei.

References:

1. Cejnar, Pavel, Jan Jolie, & Richard F. Casten. (2010). "Quantum phase transitions in the shapes of atomic nuclei." *Reviews of Modern Physics* 82.3 (2010): 2155-2212.
2. Fortunato, L. (2021). "Quantum phase transitions in algebraic and collective models of nuclear structure." *Progress in Particle and Nuclear Physics* 121 (2021): 103891.

3. Cejnar, Pavel, & Jan Jolie. (2009). "Quantum phase transitions in the interacting boson model." *Progress in Particle and Nuclear Physics* 62.1 (2009): 210-256.
4. Frank, Alejandro, et al. (2019). "Symmetry in Nuclear Physics: The Interacting Boson Model." *Symmetries in Atomic Nuclei: From Isospin to Supersymmetry* (2019): 71-102.
5. Kuprikov, V. I., & Tarasov V. N. (2019). "Change in the Shape of Nuclei in the Chains of Krypton, Strontium, Zirconium, Molybdenum, and Ruthenium Isotopes in the Relativistic-Mean-Field Approximation." *Physics of Atomic Nuclei* 82.3 (2019): 191-200.
6. García-Ramos, José Enrique, & Kristiaan Heyde. (2019). "Quest of shape coexistence in Zr isotopes." *Physical Review* C 100.4 (2019): 044315.
7. Zhang, X. Y., et al. (2023). "Nuclear charge radii and shape evolution of Kr and Sr isotopes with the deformed relativistic Hartree-Bogoliubov theory in continuum." *Physical Review* C 108.2 (2023): 024310.
8. Angeli, István, et al. (2009). "N and Z dependence of nuclear charge radii." *Journal of Physics G: Nuclear and Particle Physics* 36.8 (2009): 085102.
9. (ENSDF (2010), Nuclear Data Sheet, Retrieved from www.nndc.bnl.gov/ensdf
10. Iachello, F. (1981). "An Introduction to the Interacting boson model." *Nuclear structure* (1981): 53-89.
11. Arima, A., & Iachello F. (1978). "Interacting boson model of collective nuclear states II. The rotational limit." *Annals of Physics* 111.1 (1978): 201-238.
12. Arima, Akito. (1981). *"Interacting boson model."* Topics in Nuclear Physics II A Comprehensive Review of Recent Developments: Lecture Notes for the International Winter School in Nuclear Physics Held at Beijing (Peking), The People's Republic of China December 22, 1980-January 9, 1981. Springer Berlin Heidelberg, 1981.
13. (2020). Al-Sadi, Mohammed Abdul Kadhim Hadi, Ali Hussein F. Alnasraui, and Dhay Alaa Altbtbiey. "Mixed Symmetry States for even-even 218-224 Ra Isotopes by using (IBM-2)." *Journal of Physics: Conference Series*. Vol. 1664. No. 1. IOP Publishing, 2020.
14. Grodner, E., et al. (2022). "Examination of nuclear chirality with a magnetic moment measurement of the I= 9 isomeric state in Cs 128." *Physical Review* C 106.1 (2022): 014318.
15. Jalili-Majarshin, A., M. A. Jafarizadeh, & Fouladi, N. (2016). "Algebraic solutions for two-level pairing model in IBM-2 and IVBM." *The European Physical Journal Plus* 131.9 (2016): 337.
16. Dejbakhsh, H., A. Kolomiets, & Shlomo, S. (1995). "Structure of the even-even Kr isotopes within the interacting boson model." *Physical Review* C 51.2 (1995): 573.
17. Arima, A., & Iachello, F. (1984). "The interacting boson model." *Advances in Nuclear Physics:* Volume 13. Boston, MA: Springer US, 1984. 139-200.
18. Casten, R.F., & Warner, D.D. (1988). "The interacting boson approximation." *Reviews of Modern Physics* 60.2 (1988): 389.
19. Vallejos, O., & Barea, J. (2021). "Octupole and quadrupole modes in radon isotopes using the proton-neutron interacting boson model." *Physical Review* C 104.1 (2021): 014308.
20. Sambataro, M., et al. (1984). "On magnetic dipole properties in the neutron-proton IBA model." *Nuclear Physics* A 423.2 (1984): 333-349.
21. Sambataro, M., & Dieperink, A. E. L. (1981). "G-factors in the neutron-proton interacting boson approximation." *Physics Letters* B 107.4 (1981): 249-252.
22. Dowie, J. T. H., et al. (2020). "Table of electronic factors for E0 electron and electron-positron pair conversion transitions." *Atomic Data and Nuclear Data Tables* 131 (2020): 101283.
23. Mu, Cheng-Fu, & Da-Li Zhang. (2020). "A unified description of shape coexistence and mixed-symmetry states in 98Mo using IBM-2." *Communications in Theoretical Physics* 72.5 (2020): 055302.
24. Al-Garbawi, Ali Mahdi, & Husam Abdul-Ameer Al-Shemmari. (2016). *"The calculation of energy levels and electromagnetic transition E0, M1, E2 FOR CE and W isotopes by IBM-2."*.
25. Inci, I., et al. (2009). "Coherent state approach to the interacting boson model: Test of its validity in the transitional region." Phys*ical Review C—Nuclear Physics* 80.3 (2009): 034321.
26. Church, E. L., & Weneser, J. (1956). "Electric-monopole transitions in atomic nuclei." *Physical Review* 103.4 (1956): 1035.
27. Mohaisen, Afrah J., Saad N. Abood, & Laith A. Najam. (2021). "Electric Monopole Transitions in Nd Nuclei within IBM-2." *Egyptian Journal of Physics* 49.1 (2021): 89-100.
28. Rasmussen, John O. (1960). "Theory of E0 transitions of spheroidal nuclei." *Nuclear Physics* 19 (1960): 85-93.